

## Measurement of a CD and Sidewall Angle Artifact with Two Dimensional CD AFM Metrology

R. Dixon<sup>1</sup>, N. Sullivan<sup>2</sup>, J. Schneir<sup>1\*</sup>, T. McWaid<sup>1\*</sup>, V.W. Tsai<sup>3</sup>, J. Prochazka<sup>4</sup>, M. Young<sup>5</sup>,

<sup>1</sup>National Institute of Standards and Technology, Gaithersburg, MD 20899.

<sup>2</sup>Digital Semiconductor, Hudson, MA 01749-2895

<sup>3</sup>Dept. of Material Engineering, University of Maryland, College Park, MD 20742-4111.

<sup>4</sup>VLSI Standards, Inc., San Jose, CA 95134-2006

<sup>5</sup>Veeco-Sloan, Santa Barbara, CA 93103

\*Present Address: Tencor Instruments, Santa Clara, CA 95054

### ABSTRACT

Despite the widespread acceptance of SEM metrology in semiconductor manufacturing, there is no SEM CD standard currently available. Producing such a standard is challenging because SEM CD measurements are not only a function of the line width, but also dependent on the line material, sidewall roughness, sidewall angle, line height, substrate material, and the proximity of other objects. As the presence of AFM metrology in semiconductor manufacturing increases, the history of SEM CD metrology raises a number of questions about the prospect of AFM CD artifacts. Is an AFM CD artifact possible? What role would it play in the manufacturing environment? Although AFM has some important advantages over SEM, such as relative insensitivity to material differences, the throughput and reliability of most AFM instruments is not yet at the level necessary to support in-line CD metrology requirements. What, then, is the most useful relationship between AFM and SEM metrology? As a means of addressing some of these questions, we have measured the CD and sidewall angle of a 1.2  $\mu\text{m}$  oxy-nitride line on Si using three different techniques: optical microscopy (with modeling), AFM, and cross sectional TEM. Systematic errors in the AFM angle measurements were reduced by using a rotational averaging technique that we describe. We found good agreement with uncertainties below 30 nm ( $2\sigma$ ) for the CD measurement and  $1.0^\circ$  ( $2\sigma$ ) for the sidewall angles. Based upon these results we suggest a measurement procedure which will yield useful AFM CD artifacts. We consider the possibility that AFMs, especially when used with suitable CD artifacts, can effectively support SEM CD metrology. This synergistic relationship between the AFM and SEM represents an emerging paradigm that has also been suggested by a number of others.

**Keywords:** SPM, AFM, CD, Standards, Metrology

### 1. INTRODUCTION

Scanning electron microscopes (SEMs) are used very effectively in semiconductor metrology, despite the lack of a CD standard. Although SEM CD metrology has limitations due to effects such as material sensitivity and the proximity of other features<sup>1-3</sup>, these disadvantages are somewhat compensated for by the reliability and throughput of SEM instruments. As the presence of atomic force microscope (AFM) metrology in the semiconductor fab becomes significant, it is appropriate to consider the need and prospects for AFM CD artifacts in light of the SEM experience.

We begin by considering the potential benefits of AFM CD artifacts in terms of a qualitative Cost of Ownership model for an AFM CD metrology tool. If improved measurements increase the yield learning rate, then this is a potentially large value adding term in the cost of ownership equation for the instrument. Thus, artifacts and measurement techniques which result in improved long-term repeatability for AFM measurements are potentially of value. We observe, however, that the resulting AFM measurement need not necessarily be accurate. For example, a nominal (uncalibrated) 1  $\mu\text{m}$  oxy-nitride linewidth artifact could be used to repeatably determine a nominal width of an AFM tip. This would improve the long-term repeatability of measurements on 0.35  $\mu\text{m}$  photoresist lines. It would not be a calibration, as the 0.35  $\mu\text{m}$  CD measurements would not necessarily be accurate. However, the improved measurement repeatability, due to consistent subtraction of instrument effects (tip width, primarily), might yield a correspondingly improved return on investment for the AFM tool. Therefore, even non-ideal or uncalibrated AFM CD artifacts could play an important role in the semiconductor fab.

To examine the question of AFM CD artifact feasibility, we performed a series of measurements on a 1.2  $\mu\text{m}$  oxy-nitride line on a silicon substrate. We measured the CD and sidewall angle of this proto-linewidth sample using optical microscopy (with modeling), AFM, and cross sectional transmission electron microscopy (TEM). The AFM measurements were corrected for scanner distortions using a novel technique utilizing rotational symmetry. In this paper, we will discuss the results of this comparison, the possible implications for the future of AFM CD artifacts, and consider the potential relationship between SEM and AFM metrology in semiconductor manufacturing.

## 2. SAMPLE DESCRIPTION AND NON-AFM CHARACTERIZATIONS

The specimen which was used for our measurements is a thick-line calibration sample developed by VLSI Standards.<sup>4,5</sup> This sample consists of a roughly 1.4  $\mu\text{m}$  thick layer of oxynitride, which has been patterned to form various sized lines and spaces, on a silicon die. It was designed as a develop-inspect standard for linewidth metrology using optical microscopy. (The oxynitride is constituted to mimic the optical properties of photoresist but it has better material stability.) The line we choose for the inter-comparison of measurement techniques has a nominal width of 1.2  $\mu\text{m}$  at half the height and nominal 80 degree sidewalls. This was the smallest line available on the sample, and thus the size most useful and relevant for AFM CD metrology.

As the central goal of our work is examining the feasibility and usefulness of an AFM CD artifact, the discussion in this paper will largely focus on the AFM measurements that were performed on the sample. The comparison with the results of other measurement techniques, which are described below, serves largely to help us evaluate and better understand the AFM measurements. Optical microscopy measurements on the sample were performed by the vendor prior to the other measurements, and, after the AFM measurements were made, cross sectional TEM was performed on the sample.

### 2.1. Optical Microscopy Measurements of Linewidth Sample

An optical microscope calibration<sup>6</sup> of the sample was performed prior to its being released for other measurements. The measurement system employed for this calibration was a tuned, bright field, reflection mode optical microscope using 546.1 nm (green light) illumination (provided by mercury arc lamp and a narrowband interference filter). This system is modeled after a prototype instrument developed by Nyyssonen<sup>7</sup>, and the

methods used to analyze the data are similar to those described by Wojcik, et. al.<sup>8</sup> Values of the sidewall angle and the CD at the top, bottom, and center of the line were obtained using this system and approach. The result obtained for the sidewall angles was 80 (3) degrees (i.e. 80 +/- 3 degrees - 2 sigma). (In this paper, we shall give uncertainties in parenthesis, where this is understood to mean +/- the uncertainty given.) Linewidth values obtained were 0.99 (0.16)  $\mu\text{m}$ , 1.23 (0.08)  $\mu\text{m}$ , and 1.48 (0.16)  $\mu\text{m}$  for the CD at the top, middle, and bottom of the line respectively. The sidewall angle and CD at the middle will be the most useful for comparison with our AFM measurements. We note that for the calibration report the index of refraction was measured by ellipsometry and the thickness of the oxynitride film was derived from measurements of the relative reflectivity and phase shift of the film on silicon. The final structure height was also measured by profilometer. Discrepancies between the derived film thickness and the profilometer measurements were observed with this sample<sup>9</sup> and others similar to it.<sup>8</sup> It was believed that these differences could be the result of over etching of the silicon, a conclusion that is supported by the TEM micrograph we discuss below. As a result of this situation a reliable value of structure height cannot be taken from the calibration report. This does not affect the present work, however, as we are principally concerned with the CD measurement. In any case, we obtained an accurate value of height using AFM, and this measurement will satisfy the needs of the present work.

## 2.2. Measurements from TEM Micrograph of Linewidth Sample

After the completion of the AFM measurements, the sample was cross sectioned and TEM was performed on it. In figure 1, a TEM micrograph of the linewidth sample resulting from this analysis is shown. The basic line topography of the sample is as expected. Additionally, as noted above, over etching of the silicon substrate is apparent in the micrograph. The quantities we are interested in extracting from this micrograph are the width (at half of the height) of the line and the angles of the sidewalls. We obtained the TEM analysis from an ISO9000 certified laboratory.<sup>5,10</sup> The required calibration procedure, which involves calibration against the Si lattice spacing for high magnifications and traceability to secondary standards at lower magnifications, results in an accuracy of 5%. However, the vendor<sup>11</sup> believes it to be somewhat better than this. It is thought that effects such as lens hysteresis, electrical stability, etc. limit the accuracy to two or three percent. For the sample we are using, these effects would correspond to a starting uncertainty of 25 to 35 nm. However, if the tilt of the specimen is properly controlled when the TEM micrograph is taken, the magnification difference between two axes is expected to be less than 1%. This corresponds to an uncertainty contribution of less than 10 nm. We will exploit this situation by using the height of the line, which can be accurately measured by AFM, to calibrate the scale of the TEM micrograph. As the measurement of the sidewall angle depends only on the scales being the same along different axes, this 'calibration' procedure is useful in performing a comparison of linewidth results.

Analysis of the micrograph, to extract values of height, width, and sidewall angle, was performed by scanning the micrograph into a bitmap file. A number of points were selected along the bottom, top, and sides of the profile. Least squares lines were fit to these segments of the profile and used to extract values of the structure height, width, and sidewall angle. The height was determined by extrapolating the top and base lines (on each side) to the center of each sidewall, and the results for each side were averaged for comparison with the other techniques. Observed differences between the two sides were less than 10 nm and this disagreement is included in the uncertainty estimates. The width was determined at half the structure height, and we note that it is relatively insensitive to small variations in the selected height. Sidewall angles were determined by the differences in the inverse tangents of the base and sidewall slopes. Points along the profile were selected using three methods of edge detection. The first method used was direct human eye selection. Two edge enhancing

operators, the Roberts gradient and the Sobel function, were then applied to the image, and points were selected for both of these results. In table 1 the results of this analysis are summarized. The uncertainties ( $2\sigma$ ) given represent repeatability and algorithm error estimates only, and the width values have not been rescaled using AFM height data. The rescaling and resulting uncertainty will be discussed more when the TEM results are compared with the SXM measurements. At this point, however, it is useful to note that we are able to attain uncertainties on the order of 20 nm (two sigma) in extraction of the width from the TEM micrograph. Indeed, the level of agreement between the results extracted using the different methods suggests that this estimate may be conservative.

### 3. CHARACTERIZATION OF SAMPLE USING AFM

#### 3.1. Preliminaries and Calibration of the Veeco SXM

The AFM measurements on the sample were performed using a Veeco-Sloan SXM<sup>5</sup>, an atomic force microscope developed by Yves Martin and coworkers of IBM<sup>12</sup>. It has the capability to image feature sidewalls through the use of a flared tip and two dimensional force sensing. In this system, unlike the conventional force sensing scheme used in many AFMs, the tip position feedback is sensitive to both vertical and lateral forces acting on the tip. The SXM also has integrated capacitance-sensor metrology which enables it to perform highly repeatable measurements. These properties of the SXM system make it well suited to the applications of the semiconductor fab, and thus also make it an appropriate and suitable instrument for a test of our artifact 'calibration' scheme.

In order to perform accurate metrology of widths and heights with the SXM, it is necessary to check the calibration of the scales prior to making measurements. For this purpose, we used two additional artifacts supplied by VLSI Standards: 1.) a 935 nm step height sample, and 2.) a 'waffle' pitch-height standard with a 1.8  $\mu\text{m}$  pitch. In figure 2 we show the SXM measurements on the step height standard. Each plotted data point represents the average of results taken from nine SXM line scans. As a test of dynamic repeatability, the wafer was repositioned under the tip and the force automatically adjusted between points. The average of these points is 885.5 (1.8) nm ( $2\sigma$ ). An accurate value of the step height, 935.54 (0.6) nm ( $2\sigma$ ) was obtained at NIST using a TalyStep and master standards. From this data, we conclude that the z-axis calibration of the SXM is off by 5.65%. To test the linearity of the z-axis, we also performed measurements on a smaller (93 nm) step and found the same error in the scale factor. In figure 3 the results of SXM pitch measurements on the 1.8  $\mu\text{m}$  waffle artifact are shown. Each plotted data point represents the average of results taken from ten SXM line scans. The average of these points is 1.784 (20)  $\mu\text{m}$  ( $2\sigma$ ). Since the VLSI Standards (optical) calibration of the pitch is 1.773 (23)  $\mu\text{m}$  ( $2\sigma$ ), we conclude that the x-axis calibration of the SXM is accurate.

The geometry of the flared tip, as long as it remains stable, is not important in height or pitch metrology. However, as the apparent width of a measured line is increased by the width of the flared tip, the dimensions of the probe must be characterized in order to perform accurate metrology of widths. A 'tip characterizer' sample is supplied with the SXM. This sample, the IBM Nanoedge<sup>5</sup>, is a 'sawtooth' artifact with teeth that are estimated to be less 10 nm wide at the top. By scanning this sample it is possible to estimate the effective width of the probe to an accuracy of about 10 nm. A schematic explanation of this procedure is shown in figure 4. The apparent width of the edge near the top is due primarily to the width of the probe. A small contribution from the edge is estimated and subtracted from the apparent width. The uncertainty resulting from this procedure is

considered more below. Once the probe width has been determined, a general feature width measurement, such as that shown schematically in figure 5, can be corrected for the probe size. This correction is made using the on-line software, but a consideration of it will be important to the uncertainty analysis of our CD measurements.

Measurements of sidewall angle using the SXM are potentially affected by sources of error other than just the scale calibrations. The machine coordinate frame realized by the scanner system may not represent an orthonormal system. Measurements of sidewall angle would be affected if, for example, the z-axis were not at right angles to the x-y scan plane. We have developed a method for eliminating some types of scanner errors that utilizes rotational symmetry. The approach is motivated by the work of Estler<sup>13</sup>, in which a reversal was used to correct for straightedge errors in a coordinate measurement machine (CMM). As a more detailed description of our method and details of its application will be given elsewhere<sup>14</sup>, we will restrict ourselves here to a more general discussion.

The basic idea behind the reversal method, shown in figure 6, is that by averaging angles measured in opposite orientations, certain scanner metrology errors can be reduced. In figure 7, averaging of the sidewall in opposite orientations with actual SXM data is shown. It is possible to show that this method eliminates (to first order) certain *repeatable* scanner metrology errors. We let  $\hat{x}, \hat{y}, \hat{z}$  consist of ortho-normal axes, and let z be the axis of rotation. Next, we define a mapping  $M\{x,y,z\} = \{i(x,y,z), j(x,y,z), k(x,y,z)\}$  from the ideal orthonormal coordinate system to the distorted machine coordinate system of the SXM. In this definition, x,y,z are considered to be dimensionless variables giving the position as a fraction of the entire scan range. If R is defined as the operator which rotates 180° about the z axis, then we have  $R\{x,y,z\} = \{-x,-y,z\}$ . The correction procedure we will use consists of these steps: (1) image a sample in the SXM, (2) rotate the sample 180°; (3) image the sample again, and (4) average the results. Mathematically, this may be represented by the expression:

$$\frac{M+R^{-1}MR}{2}\{x,y,z\} \quad (1)$$

To determine the extent of the cancellation of error terms in this expression, we can define the three machine error functions:  $f(x,y,z) = i(x,y,z) - x$ ,  $g(x,y,z) = j(x,y,z) - y$ , and  $h(x,y,z) = k(x,y,z) - z$ . If we sensibly choose the ideal coordinate system to be one that is 'close' to the distorted machine system, then these error functions can be treated as small slowly varying functions of x, y, and z. A Taylor series expansion can be performed, and a straightforward evaluation<sup>14-16</sup> of expression (1) leads to the conclusion that repeatable scanner metrology errors, except for calibration of the x and z axes and the coupling of x and y axes, are canceled to first order. We will utilize this cancellation in the analysis of the sidewall angle data.

### 3.2. Analysis and Discussion of SXM Measurements on Linewidth Sample

A representative line scan from the SXM data on the VLSI linewidth sample is shown in figure 8. This scan reveals the same basic profile of the line as the TEM micrograph, but also has some instrument artifacts that must be noted. First, the apparent width of the lines is increased (dilated) by the width of the flared probe. The corners at the top and bottom do not represent the actual line because the imaging point on the probe is changing during these portions of the scan. Additionally, the top and bottom surfaces may appear smoothed out due to the shape of the probe, which is essentially flat on the bottom. The properties of the sample that we wish to

determine from the SXM data are the structure height, structure width or CD, and the angles of the sidewalls. In table 2, the results obtained from the SXM data are summarized, and, where appropriate, the values obtained from the other measurements are given for comparison. As discussed below, we used both the on-line analysis software and off-line analysis of the data files to accomplish these determinations.

The height of the structure was determined using the on line analysis software as the data were collected. This algorithm excludes 10% of the profile around the corners and determines the difference between the average z value of the upper and lower surfaces. Thirteen different results, each representing the average of 10 line scans, were averaged to obtain 1410.6 (12.2) nm ( $2\sigma$ ). As the repeatability of the SXM on a uniform sample is better than 1 nm, the observed variation is due almost exclusively to the non-uniformity of the sample. This is fairly consistent with a close inspection of the TEM micrograph, which indicates that the non-uniformity on the top of the oxynitride structure is at least on the order of 10 nm. In fact, residuals from our fits to the top of the profile extracted from the TEM micrograph revealed the maximum peak to valley variation to be roughly 25 nm. This variation in the sample is potentially important, because it can lead to a methods divergence uncertainty between the SXM measurements and profiles extracted from the TEM micrograph. To analyze the TEM data, we extracted points along the profile and fit a line through them, a method that treats all the points equally. However, the flared probe that the SXM uses is very blunt on the bottom (essentially a ~250 nm flat). Hence the SXM probe does not sample depressions in the surface which have spatial wavelengths of (roughly) less than 250 nm. In other words the probe tends to 'ride' on the surface asperities and, therefore, the points on the sample are not all weighted equally. From the TEM micrograph of figure 1, we can see that the upper (oxynitride) surface of the line is somewhat less smooth than the lower (etched Si) surface. This means that while the SXM and TEM sample approximately the same bottom surface, the SXM will 'see' a higher average value of the upper surface than the TEM. The use of the SXM height measurement to rescale the TEM data thus introduces an error. Fortunately, this effect is one sided (in this case, the SXM measured height is only increased by the effect) and we can also see that it should be fairly small. Based upon the maximum peak to valley variation in the TEM data, it can be reasonably assumed that the average offset introduced in the SXM data should be no more than 10 nm. This would correspond to a 9 nm error in the rescaled TEM width value. A method of reducing this offset would be to filter the TEM profile with a 'blunt tip' envelope. However, since the estimated size of the offset is smaller than the dominant sources uncertainty, we will simply include it in the uncertainty budget by taking 10 nm as the estimated  $2\sigma$  limit. A systematic uncertainty of 1.5 nm ( $2\sigma$ ) resulting from the calibration of the z-scale was also added in quadrature to give the final height and uncertainty of 1410.6 +12.3/-15.8 nm ( $2\sigma$ ).

The width or CD of the oxynitride structure was also determined using the on line analysis software as the SXM data were collected. The algorithm finds the points at half of the height (on each side), averages the x values around these points at +/- 3% of the sidewall height. The CD is given by the x separation between these two averages. This averaging procedure reduces the effect of any local variations along the sidewalls. Thirteen different results, each representing the average of 10 line scans, were averaged to obtain 1229.1 (11.4) nm ( $2\sigma$ ). As was the case with the height measurements, this spread in the values is due primarily to sample variation. The major additional source of uncertainty in the measurement is due to the correction for the width of tip. This correction is made in the software and is already included in the average given above. The width to use in the correction is determined by scanning the tip characterizer sample (IBM NanoEdge) prior to taking data on the linewidth specimen. The edges on this sample have ridges that have a nominal radius of curvature at the top of 5 nm +/- 2 nm. Hence, the width of the probe would be determined by subtracting about 10 nm from the

apparent width (near the top) of the ridge as measured by the SXM. Potential sources of uncertainty resulting from this procedure are variations in the dimensions of the NanoEdge and the possibility that the effective imaging points on the probe while scanning the NanoEdge are not the same as those while scanning the specimen of interest. Since the sidewalls of our linewidth sample are almost as steep as those of the NanoEdge, we believe the latter contribution to be fairly small, probably less than 5 nm. Using the same probe, we scanned several regions of the NanoEdge and observed<sup>17</sup> peak to peak variations of about 15 nm in the apparent width of the ridges. This clearly suggests that the ridges are wider than 10 nm in some locations. It seems probable that wear of NanoEdge at least partially accounts for this variation. In view of these observations and the nominal dimensions of the artifact, we have decided to treat this source of uncertainty by assuming that the ridge contribution to the apparent width is  $10 +10/-5$  nm. If these uncertainty bounds are taken to be approximately  $1\sigma$  limits, then the extracted width of the probe has a  $+10/-20$  nm ( $2\sigma$ ) uncertainty. The probe width used for the CD data we took was 226.0 nm. We obtained a final SXM CD value and uncertainty of  $1229.0 +24/-16$  nm ( $2\sigma$ ), including (in quadrature) all of the uncertainty sources discussed above.

The sidewall angles of the oxynitride structure were measured at two orientations (180 degree rotation between them) and averaged, as discussed in the previous section. Analysis of the data to determine sidewall angles was conducted off-line. Data were taken at nine locations in the first orientation and four in the second (the thirteen total data sets previously discussed). Excluding the transition corners at the bottom and top, least squares lines were fit to the sidewalls and baseline (similar to the TEM analysis). Cut-offs were chosen such that the results were stable. All profiles were averaged for each orientation. Variation in the slopes of the fitted lines is the major source of random error. This was estimated from the fitting procedure to be about 0.6 degrees ( $2\sigma$ ). There is also a systematic scanner metrology error, as evidenced by the large difference in the measured sidewall angle in the two orientations. However, when the results in the two orientations are averaged, this error is greatly reduced. We have taken the random uncertainty in the averages of table 2 to be 0.6 degrees ( $2\sigma$ ), but have not included any estimate of the remaining systematic error. We will consider this matter in the next section, when we discuss the comparisons of the results. Finally, we note that there is an approximately 3.5 degree difference (3.7 degrees for sidewall A and 3.2 degrees for sidewall B) in the measured sidewall angle between the two orientations. This offset corresponds to the slope difference that was apparent in figure 7. One possible explanation for this, as shown in figure 9, is that the z axis is not at right angles to the x-y scan plane. When a correction for this was entered into the analysis software, after completion of the present work, the performance of the instrument in subsequent measurements was enhanced.<sup>16</sup>

#### 4. DISCUSSION AND COMPARISON OF RESULTS

As discussed earlier, since the scale of the TEM micrograph has up to 5% uncertainty, we have taken the SXM measured structure height of  $1410.6 +12.3/-15.8$  nm ( $2\sigma$ ) as accurate and used this value to rescale the TEM results for the measurement of structure width. The TEM height value used to determine the rescaling factor was taken to be the average of the result of the three profile extraction methods. This value, shown in table 2 was 1345 (10) nm ( $2\sigma$ ), where the uncertainty is dominated by systematic uncertainties in profile extraction. This procedure, of course, leaves us without an independent measurement of structure height to compare with the SXM. In future experiments, we hope to obtain independent stylus measurements of the structure height.

The final average SXM measured CD at half height is  $1229.0 +24/-16$  nm ( $2\sigma$ ). This result is in good agreement with the optically measured value of 1230 (80) nm ( $2\sigma$ ), but it has a substantially smaller uncertainty. It is also

in good agreement with the rescaled TEM value of  $1221 \pm 26/-28$  nm ( $2\sigma$ ). This result, shown in table 2 along with the result before rescaling, is obtained from an average of the three different profile extraction methods. The uncertainty of this average TEM value includes the (conservative) estimate of the profile extraction contribution of 20 nm ( $2\sigma$ ), the rescaling contribution of 14 nm ( $2\sigma$ ), and a systematic 10 nm ( $2\sigma$ ) contribution for possible difference (conservative estimate of 1%) of the TEM magnifications along the two orthogonal directions. It also includes an estimate of the methods divergence between the TEM and SXM in the sampling of the upper surface. As was discussed in the last section, the size of this effect should not exceed about 9 nm, and it is a one-sided source of uncertainty. We have treated it, therefore, by adding a  $+0/-9$  nm ( $2\sigma$ ) contribution in quadrature to obtain the final TEM width uncertainty of  $+26/-28$  nm ( $2\sigma$ ).

The orientation-averaged results for the two sidewall angles of 78.8 (0.6) degrees ( $2\sigma$ ) for sidewall A and 79.7 (0.6) degrees ( $2\sigma$ ) for sidewall B are in good agreement with the less accurate optically measured value of 80 (3) degrees ( $2\sigma$ ). As shown in table 2, the SXM values are also in good agreement with the method-averaged TEM results of 78.4 (1.0) degrees ( $2\sigma$ ) and 79.5 (1.0) degrees ( $2\sigma$ ), where the uncertainties are due primarily to extraction. There is a small systematic contribution of less than 0.3 degrees resulting from the possible difference in magnification along different axes. We are not certain about the correspondence of sidewall identification between the TEM and SXM measurements, but the agreement is satisfactory either way. Perhaps the most useful interpretation is to average the two TEM sidewalls to obtain 79.0 (1.0) degrees, which is in agreement with both SXM results. Finally, we have not yet investigated possible remaining sources of systematic error in the scanner metrology that could affect sidewall angle measurements. We do not yet know what limits non-repeatable errors and higher order terms in the expansion of equation (1) will place on these measurements. Our objective is to measure sidewall angles with an accuracy of roughly one degree, and the level of agreement in the present work indicates that this goal is realistic.

We conclude this section by considering the outlook for AFM metrology that is suggested by the level of agreement achieved in the present work. It is generally understood that AFM measurements can suffer from a variety of adverse effects involving tip or cantilever distortions which could make accurate metrology challenging. In conventional AFM, particularly in the contact mode, buckling of the cantilever, due to lateral forces acting on the tip, can produce both false height contrast<sup>18-20</sup> and altered apparent widths<sup>20,21</sup>. The magnitude of observed lateral forces is often increased by the water layers on the surfaces under conditions of high humidity.<sup>20</sup> Lateral forces may also cause flexing of high aspect ratio probes.<sup>22</sup> In the present work, however, the AFM used operates in a 'non-contact' mode, sensing attractive forces between the probe and sample, and it is sensitive to forces in both the lateral and vertical directions.<sup>12</sup> Furthermore, our instrument is operated in a clean room under conditions of low relative humidity. For these reasons, this AFM could be expected to suffer less than conventional AFMs from tip or cantilever bending effects. The success of the present work strongly suggests that this is the case and it implies a positive outlook for this type of AFM CD metrology.

## 5. CONCLUSIONS AND FUTURE WORK

The accuracy of AFM CD measurements may ultimately approach the nanometer level, and, in the future, the throughput of CD AFMs may be expected to increase by up to an order of magnitude.<sup>23</sup> Nevertheless, it seems unlikely that AFMs will soon displace SEMs in the semiconductor process line. Rather, as others have suggested<sup>23-26</sup>, it seems probable that AFMs will complement and support SEM CD metrology for both in line

and process development purposes. The throughput of the CD AFM is already adequate for process development and production support.<sup>27</sup> Future improvements in AFM metrology will further increase the viability of this application. For in-line metrology, the CD AFM is also beginning to play an important supportive role to the SEM. The material sensitivity and proximity effects of an SEM require that an in-house CD standard be 'on product'. As the material sensitivity of AFMs is much smaller than that of SEMs, the CD AFM could be used to transfer the accuracy of a more stable dimensional standard to an 'on product' reference structure.

In consideration of this new paradigm and the results of the present work, we suggest a measurement procedure which will yield useful AFM CD artifacts. For this purpose, we have obtained a set of samples similar to the sample used in the present work. Using the techniques for accurate AFM metrology that we have developed in this work, we plan to establish the uniformity of these artifacts with respect to CD and sidewall angle. The step height of the samples will then be established accurately using AFM and/or stylus measurements. Some of the samples will be cross sectioned and examined in the TEM. The structure height will determine the scale on the TEM micrograph. The remaining samples will thus be well characterized and can serve as useful CD AFM transfer standards for production support. Once we have completed this measurement procedure, we plan to use the characterized artifacts in round robin experiments with other SXM users and with other measurement techniques.

#### **ACKNOWLEDGMENTS**

This work was largely supported by the National Semiconductor Metrology Program (NSMP) at NIST. We wish to thank T. Vorburger, D. Yaney, E. C. Teague, D. A. Swyt, J. Villarrubia, M. Postek, J. Potzik, and R. Silver of NIST for helpful discussions and encouragement. Finally, we thank R. Anderson of the IBM Analytical Services Group for his effort in preparing the X-TEM micrographs we used in this work.

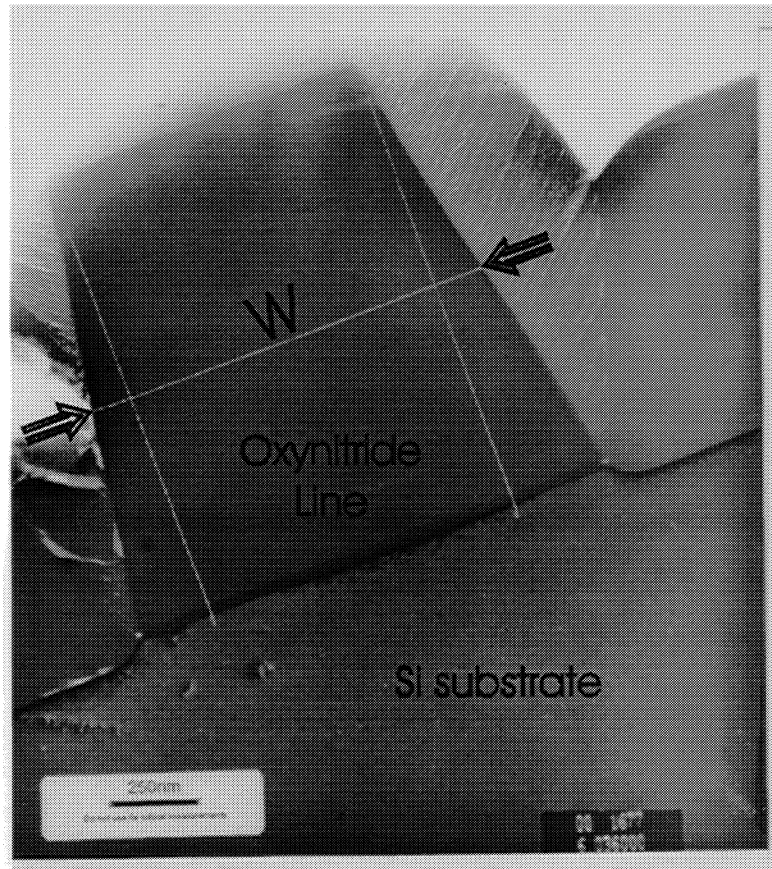


**Figure 1.** Cross sectional TEM micrograph of VLSI oxy-nitride on Si linewidth sample. The two ‘vertical’ lines are approximate perpendiculars, and the arrows indicate the width at about half of the line height. This is CD value that we are interested in comparing to the SXM result.

Analysis Method: ----- Measured Quantity:	Unfiltered Image	Robert’s Filtered Image	Sobel Filtered Image
Structure Height (nm)	1348 (20)	1344 (20)	1343 (20)
Structure Width (nm)	1159 (20)	1169 (20)	1168 (20)
Left Sidewall Angle	80.2 (1.0)	79.8 (1.0)	78.5 (1.0)
Right Sidewall Angle	78.4 (1.0)	78.3 (1.0)	78.5 (1.0)

**Table 1.** Values extracted ( $2\sigma$  uncertainties) from analysis of TEM micrograph in figure 1.

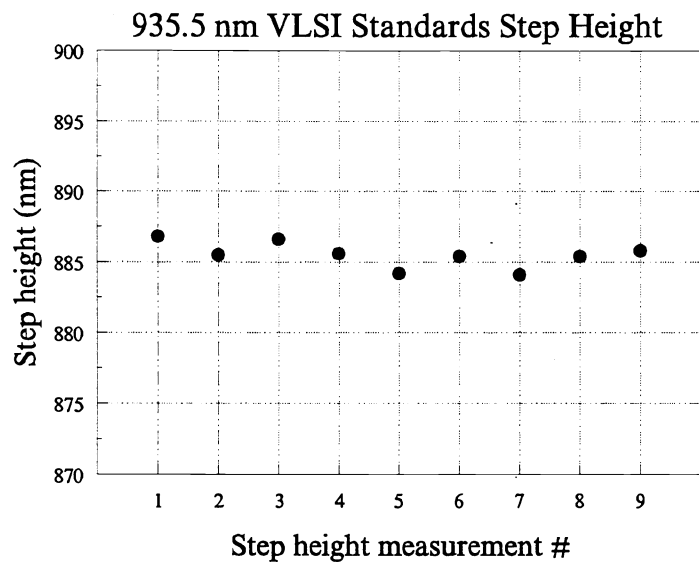


**Figure 2.** Check of Z-Magnification: each point represents the average of 9 line scans taken at ~ 1 Hz. Between points the wafer was repositioned under the tip and the force was automatically readjusted to test dynamic repeatability. The result is 1.8 nm  $2\sigma$ .

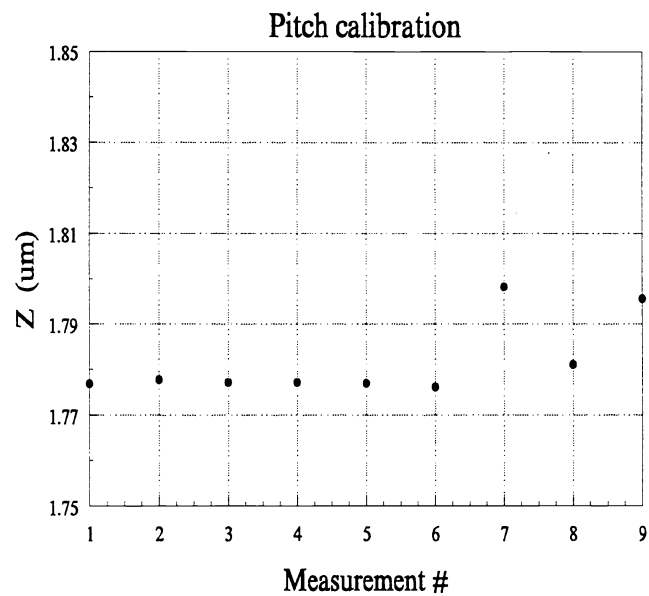


**Figure 3.** Check on X magnification (pitch): SXM result is  $1.784 \pm .020 \mu\text{m}$  ( $2\sigma$ ), VLSI Standards (using optical calibration) result is  $1.773 \pm .023 \mu\text{m}$  ( $2\sigma$ ).

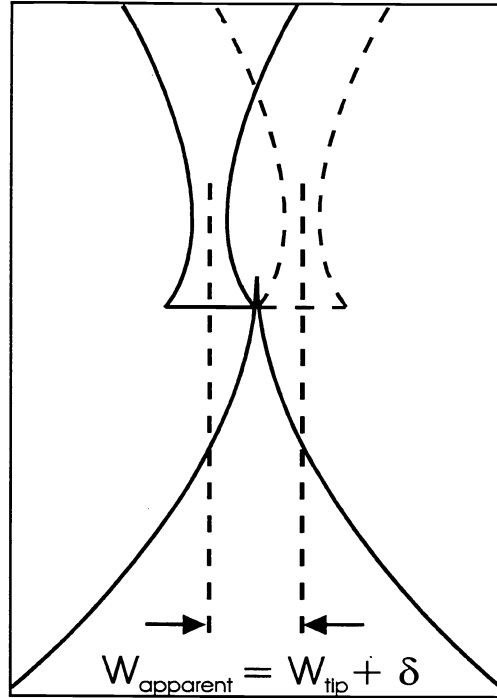


**Figure 4.** Schematic of flared SXM probe scanning over NanoEdge: the apparent width at the top is due primarily to the width of the probe.

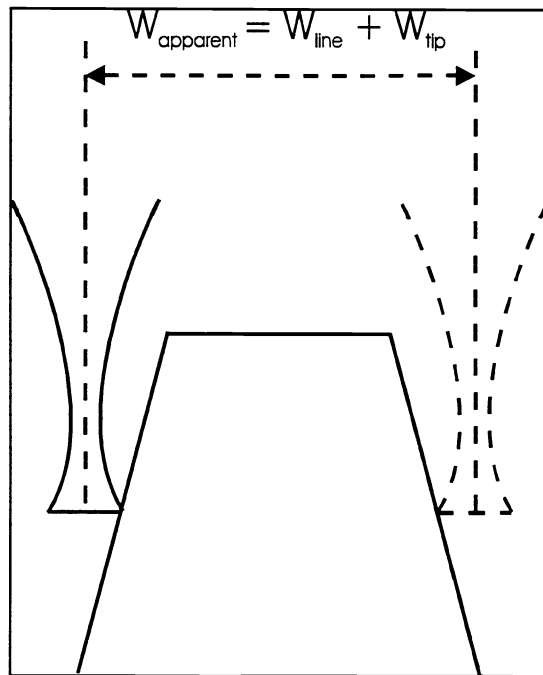


**Figure 5.** Schematic of SXM probe scanning oxynitride linewidth sample: the apparent width, due to both the line and probe, can be corrected for the tip width as determined from the NanoEdge.

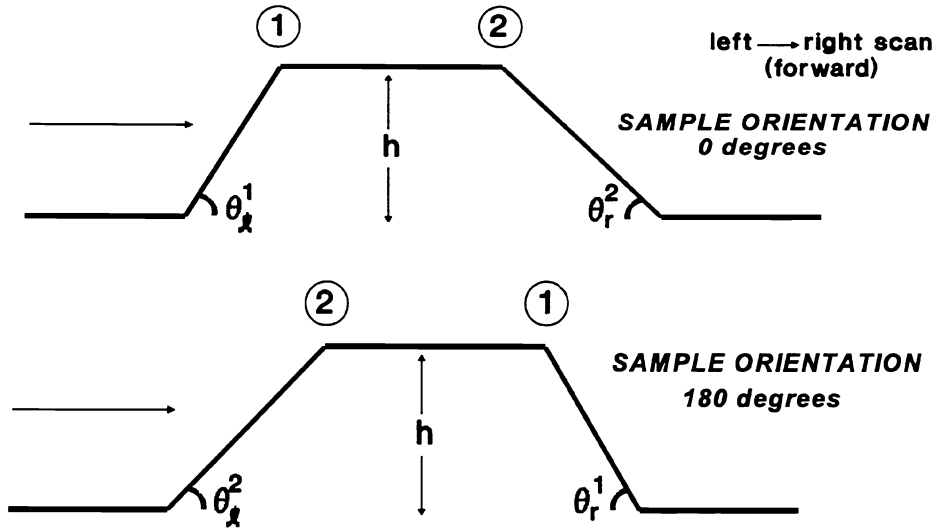


**Figure 6.** Method for improving sidewall angle measurements: by averaging the same sidewall imaged in two orientations all repeatable scanner metrology errors are, to first order, eliminated except for x-axis calibration, z-axis calibration, and x-y coupling. The sample sides are labeled '1' and '2', and the orientation of the sides with respect to the forward scan direction is labeled L or R.

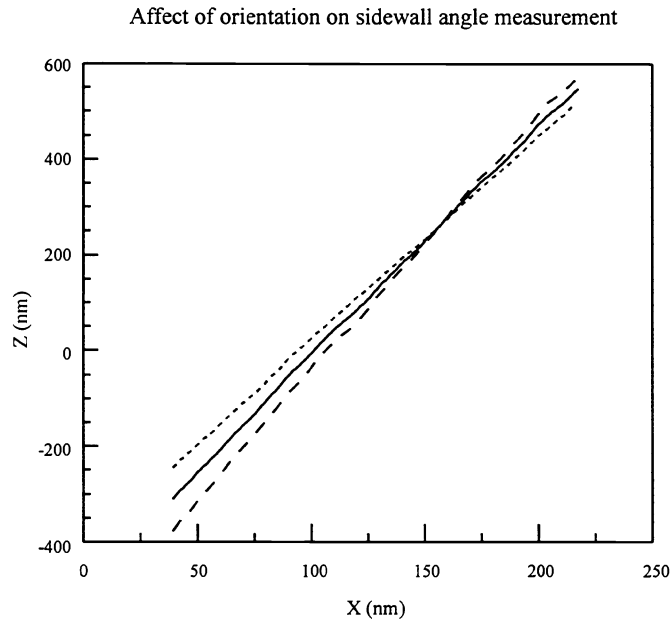


**Figure 7.** Implementation of rotational averaging - the plot shows the same sidewall in both orientations and the averaged result. There is a difference in the slopes, showing the presence of a systematic error in angle metrology

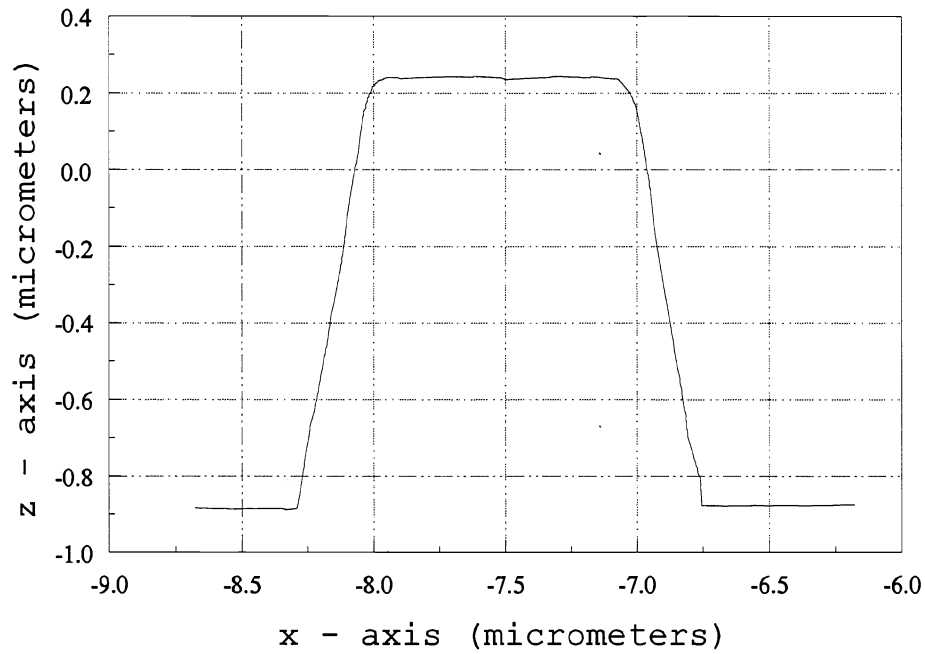


**Figure 8.** Line profile of VLSI oxynitride linewidth sample extracted from SXM data; note that the data includes the increased apparent width due to the size of the SXM probe.

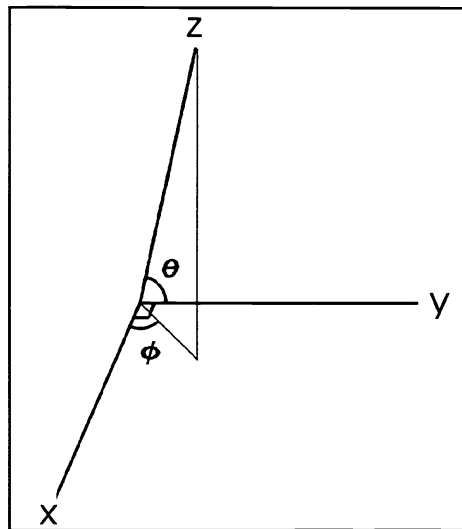


**Figure 9.** The differences in the measured sidewall angles in the two orientations are  $3.7^\circ$  and  $3.2^\circ$ , as shown in figure 5. One possible explanation for this is that the z-axis is not normal to the x-y plane, but is instead at the angles  $\theta = -1.7^\circ$  and  $\phi = 90^\circ$  with respect to it.

Analysis Method: ----- Measured Quantity:	SXM Measurement	TEM Result	Optical Microscopy
Structure Height (nm)	1410.6 +12.3/-15.8	1345 (10)	-----
Structure Width (nm)	1229.0 +24/-16	1165 (20) 1221 +26/-28 (rescaled)	1230 (80)
Sidewall A Angle (1st orientation)	76.9 (0.6)	-----	-----
Sidewall A Angle (2nd orientation)	80.6 (0.6)	-----	-----
Sidewall A Angle (Average)	78.8 (0.6)	78.3 (1.0)	80 (3)
Sidewall B Angle (1st orientation)	81.3 (0.6)	-----	-----
Sidewall B Angle (2nd orientation)	78.1 (0.6)	-----	-----
Sidewall B Angle (Average)	79.7 (0.6)	79.8 (1.0)	80 (3)

**Table 2.** Comparison table of SXM Measurements with other results. All uncertainties are  $2\sigma$ . The TEM results given are the averages of the results using the three different extraction methods.

## REFERENCES

1. M. T. Postek, *J. Res. Natl. Inst. Stand. Technol.* **99**, 641 - 671 (1994).
2. M. T. Postek, A. E. Vladar, S. Jones, W. J. Keery, *SPIE Proceedings* **1926**, 268-286 (1993).
3. M. T. Postek, A. E. Vladar, S. Jones, W. J. Keery, *J. Res. Natl. Inst. Stand. Technol.* **98**, 447 - 467 (1993).
4. VLSI Standards Inc., San Jose, CA 95134-2006.
5. Certain commercial equipment is identified in this report in order to describe the experimental procedure adequately. Such identification does not imply recommendation or endorsement by NIST, nor does it imply that the equipment identified is necessarily the best available for the purpose.
6. J. J. Prochazka, VLSI Standards calibration report on sample SN 1209-015-004 (1991).
7. D. Nyssonen, NISTIR 88-3808, 1989.
8. G. L. Wojcik, J. Mould Jr., R. J. Monteverde, J. J. Prochazka, and J. R. Frank Jr, *SPIE Vol. 1464*, pp. 1 - 17, (1991).
9. J. J. Prochazka, private communication, 1996.
10. IBM Analytical Services Group, Hopewell Junction., NY.
11. Ronald Anderson, IBM Analytical Services Group, private communication, 1995.
12. Y. Martin and H. K. Wickramasinghe, *Applied Physics Letters* **64** (19), 2498 (1994).
13. W. T. Estler, *Optical Engineering* **24** (3), 372 (1985).
14. R. Dixon, N. Sullivan, in preparation for *J. Res. Natl. Inst. Stand. Technol.* (1996).
15. J. Schneir, T. McWaid, R. Dixon, and N. Sullivan, presented at 42 AVS Symposium (1995).
16. N. Sullivan, presented at SXM users conference, Austin, TX, Oct. 25, 1995.
17. R. Dixon and N. Sullivan, unpublished results, 1996.
18. G. Meyer and N. M. Amer, *Applied Physics Letters* **57**, 2089 (1990).
19. A. J. Den Boeff, *Rev. Sci. Instrum.* **62**, 88 (1991).

20. T. Thundat, R. J. Warmack, D. P. Allison, L. A. Bottomley, A. J. Lourenco, T. L Ferrell, *J. Vac. Sci. Technol. A* **10**, 630 (1992).
21. J. O. Tegenfeldt, L. Montelius, *Applied Physics Letters* **66** (9), 1068 (1995).
22. D. A. Grigg, P. E. Russell, J. E. Griffith, *J. Vac. Sci. Technol. A* **10**, 680 (1992).
23. Y. Martin, H. K. Wickramasinghe, *J. Vac. Sci. Technol. B* **13**, 2335 (1995).
24. N. Sullivan, NISTIR 5752, pp. 55-60, 1995.
25. R. M. Feenstra and J. E. Griffith, in *Semiconductor Characterization: Present Status and Future Needs*, pp. 295-307, 1996.
26. J. E. Griffith, private communication, 1995.
27. G. Vachet, M. Young, *Solid State Technol.* Vol. 38, No. 12, pp. 57-62, Dec. 1995.